BASIC SCIENCE

Nanomedicine: Nanotechnology, Biology, and Medicine
21 (2019) 102052

Original Article

nanomedjournal.com

Engineered nanomedicine for neuroregeneration: light emitting diode-mediated superparamagnetic iron oxide-gold core-shell nanoparticles functionalized by nerve growth factor

Muzhaozi Yuan, MS[a], Ya Wang, PhD[a,*], Yi-Xian Qin, PhD[b]

[a]*J. Mike Walker '66 Department of Mechanical Engineering, Texas A&M University, College Station, TX*
[b]*Department of Biomedical Engineering, Stony Brook University, Stony Brook, NY*

Revised 4 June 2019

Abstract

This paper reports nerve growth factor functionalized superparamagnetic iron oxide–gold core-shell nanoparticles (NGF-SPIO-Au NPs), an engineered nanomedicine for non-invasive neuron regeneration when irradiated by a low-intensity light-emitting diode (LED). NGF-SPIO-Au NPs of 20 μg/ml, were tested on PC-12 neuron-like cells, irradiated by LEDs (525 nm, 1.09, 1.44, and 1.90 mW/cm^2). A remarkable Ca^{2+} influx was detected in differentiated PC-12 cells treated with NPs, irradiated by LED of 1.90 and 1.44 mW/cm^2 with great cell viability (>84%) and proliferations. The strong heat generated through their plasmonic surface upon LED irradiation on NGF-SPIO-Au NPs was observed. For cells treated with LED (1.90 mW/cm^2) and NGF-SPIO-Au NPs, a dramatic enhancement of neuronal differentiation (83%) and neurite outgrowth (51%) was found, and the upregulation of both the neural differentiation specific marker (β3-tubulin) and the cell adhesive molecule (integrin β1) was observed by the reverse transcription-polymerase chain reaction and western blot analysis.

Key words: Light emitting diode; NGF-SPIO-au nanoparticles; Nerve regeneration; Calcium influx; Photothermal effect

Engineered nanoparticles (NPs) mediated by external stimuli have attracted accumulative attentions in nanomedicine for non-invasive or less invasive therapeutics. In particular, gold (Au) nanoparticles have been used as a mediator to induce light-based neuro-stimulation through photothermal effect from localized surface plasmon resonance (LSPR).[1] Superparamagnetic iron oxide (SPIO) NPs are also extensively studied as the nano drug carriers of nerve growth factor (NGF) because of their strong magnetic properties that can be used to enhance the neurite growth and direct the neurite orientation mediated by external magnetic fields (MFs).[2–4] Adding a protective and functional shell of Au on SPIO core to avoid aggregation[5] and enhance the biocompatibility,[6] SPIO-Au core-shell NPs possess very unique and attractive features integrating the magnetic properties of SPIO and the LSPR properties of Au into one single nanoplatform,[7–9] and therefore exhibit strong potential for many multimodal biomedical applications, such as the targeted drug delivery,[10,11] photo induced/magnetic hyperthermia[12–14] and imaging-assisted cancer treatment.[15,16]

However, among these applications, there has been no attempt to use NGF functionalized superparamagnetic iron oxide–gold core-shell (NGF-SPIO-Au) NPs to modulate neuronal activities under photostimulation. In comparison with other traditional stimuli such as electrical stimulation,[20] photostimulation is considered non-invasive and relatively harmless.[17–19] In comparison with other types of nanomedicine, NGF-SPIO-Au NPs have their unique advantages for brain therapeutics. First of all, the gold shell can help regulate neuronal functionality since the plasmonically induced heat activates temperature-sensitive channels in neurons[21] for

Abbreviations: LED, light emitting diode; NGF-SPIO-Au NPs, nerve growth factor functionalized superparamagnetic iron oxide–gold core-shell nanoparticles; RT-PCR, reverse transcription-polymerase chain reaction; NPs, nanoparticles; Au, gold; LSPR, localized surface plasmon resonances; SPIO, superparamagnetic iron oxide; MFs, magnetic fields; NGF, nerve growth factor; TBI, traumatic brain injury; ATCC, American Type Culture Collection; HS, heat-inactivated horse serum; FBS, fetal bovine serum; PLL, poly-L-lysine; CCK-8, cell counting kit-8; DPBS, Dulbecco's phosphate-buffered saline; TBS, Tris-buffered saline; ANOVA, analysis of variance; F-actin, filamentous actin; ABP, actin-binding proteins; PCR, polymerase chain reaction.

The authors declare no conflict of interest.

*Corresponding author.

E-mail addresses: muzhaozi.yuan@tamu.edu, (M. Yuan), ya.wang@tamu.edu, (Y. Wang), yi-xian.qin@stonybrook.edu. (Y.-X. Qin).

https://doi.org/10.1016/j.nano.2019.102052
1549-9634/

excitation[22] and inhibition[23] of action potentials. Such a photothermal effect is also believed to regulate Ca^{2+} level,[24] which is critical for transmitting neuronal signals between neurons,[25,26] and for regulating cytoskeleton growth behaviors via phosphorylation.[27] Besides, the effective loading of therapeutic molecule (like NGF) and the magnetic property enabled the usage of magnetic force guided drug delivery. Our team has recently synthesized NGF-SPIO-Au NPs using a facile method and proved their stimulation impact on neuronal growth and differentiation under dynamic magnetic fields.[4,28] However, how this nanomedicine responds to photostimulation, an advantageous non-invasive tool to regulate neuronal activities and promote nerve regeneration, is still unknown.

Traditional photostimulation strategies rely on laser sources which could induce potential tissue damages, often require a high-voltage power supply, and are costly.[22] As an emerging alternative to a laser,[13] light emitting diode (LED) is portable, cheap, consumes little power, and has negligible human and environmental toxicity.[29–33] It has shown potentials for improving cognition on patients with chronic and traumatic brain injury (TBI).[34] The effect of 940 nm LED on sciatic nerve regeneration was also reported on rats,[35] which showed improved morphofunctional sciatic nerve recovery with phototherapy after nerve damage. However, LED has not been used as a light source to irradiate and activate plasmonic NPs, especially NGF-SPIO-Au NPs for regulating neurological functions through plasmonically-generated heat.

To overcome the current limitations of photobiostimulation and to investigate an innovative and non-invasive nerve regeneration therapeutic strategy, in this work, we used low-intensity LEDs (<2 mW/cm^2) to irradiate NGF-SPIO-Au NPs of 20.8 diameter and 20 μg/ml, a promising nanomedicine, and examined their molecular and cellular effect on PC-12 cells. Temperature assessment of LED-irradiated NPs proved the strong photothermal effect of NGF-SPIO-Au NPs and the temperature equilibrium was achieved after 25–30 minutes of heating. Therefore, we set 30 minutes as the duration time of LED treatment that is sufficient to stimulate neuronal activities via plasmonically-generated heat. The morphological evaluation of LED irradiated NGF-SPIO-Au NPs at the intensity of 1.90 mW/cm^2 on enhanced neuronal differentiation and neurite growth of PC-12 cells was performed through quantitative analysis. Using calcium imaging and molecular analysis through the reverse transcription-polymerase chain reaction (RT-PCR) and western blot assay, we further examined how LED-irradiated NGF-SPIO-Au NPs interacted with the calcium level and proteins/genes related to neurite outgrowth and neural differentiation, such as the neural specific marker, β3-tubulin protein which is known as an essential element to form microtubules,[36] and the cell adhesive molecules, integrin β1, which is important to the PC-12 cell attachment on substrate and the neurite extension.[37]

Methods

Preparation of NGF-SPIO-Au NPs

SPIO-Au NPs were first synthesized using the seed growth method and then functionalized with NGF at the mass ratio of 14:1 (NPs:NGF). Detailed procedures about the synthesis of SPIO-Au NPs and the functionalization of NGF are available in our previous publication.[4] The as-synthesized NGF-SPIO-Au NPs in the diameter of 20.8 nm were directly used in the following experiments without any further purification.

Cell culture

PC-12 cells (from rat pheochromocytoma) obtained from American Type Culture Collection (ATCC) were cultured in growth medium composed of ATCC modified RPMI1640 medium supplemented with 10% heat-inactivated horse serum (HS), 5% fetal bovine serum (FBS) and 1% penicillin–streptomycin (medium and supplements were purchased from Gibco). Cells were seeded and cultured in poly-L-lysine (PLL, P4707, Sigma-Aldrich) pre-coated Petri dishes in a humidified incubator under a 5% CO_2 atmosphere at 37 °C. To induce cell differentiation, PC-12 cells were cultured in serum-reduced medium (1% heat-inactivated HS and 0.5% FBS).

Cytotoxicity evaluation

To evaluate the cell viability of LED irradiation, the cell counting kit-8 (CCK-8, Sigma-Aldrich) was used at first. PC-12 cells were seeded into PLL-coated 96-well tissue culture plates at a density of $2*10^3$ cells/well with growth medium. After 24 hours of incubation, the medium was replaced by fresh medium containing NGF-SPIO-Au NPs at the concentrations of 0, 1, 5, 10 and 20 μg/ml. On each day, cells were exposed to LED irradiation (wavelength: 525 nm, maximum intensity: 1.90 mW/cm^2 (LIU525B, Thorlabs Inc., Newton, NJ)) at different time periods (1 min, 10 min, 30 min and 1 h). Cells without treating with LED irradiation or NPs were cultured as control groups. After 1, 3 and 5 days of incubation, the media were replaced by fresh media and 10 μl of CCK-8 solution was added to each well and followed by the incubation of the plates for 2 hours at 37 °C. The absorbance was measured using a microplate reader (SpectraMax i3x, Molecular Devices, LLC, San Jose, CA) at the wavelength of 450 nm.

To further evaluate the cytotoxicity of LED irradiation at different intensities, PC-12 cells were seeded into 24-well plates coated with PLL and incubated for 1 day. Then the cells were washed with Dulbecco's phosphate-buffered saline (DPBS) and incubated with NGF-SPIO-Au NPs at the concentrations of 5, 10 and 20 μg/ml. On each day, cells were exposed to LED irradiation for 30 minutes at 3 different light intensities (1.90, 1.44 and 1.09 mW/cm^2), which were regulated by using multilayers of the light diffuser films (Matte 1 sided, Inventables Inc., Chicago, IL). Cells without NPs were cultured as control group. After 1, 3 and 5 days, cells were dislodged from the dish, centrifuged and dispersed in the growth medium. Cells were then stained with 0.4% Trypan blue solution (Gibco, Grand Island, NY) and examined through a hemocytometer (Bright-Line™ and Hy-Lite™ Counting Chambers, Hausser Scientific Inc. Horsham, PA).

Regulation of neurite growth by LED irradiation

PC-12 cells were seeded in PLL pre-coated Ibidi Petri dishes (D: 35 mm). After 24-hour incubation in the serum-reduced medium, cells were treated with NGF-SPIO-Au NPs at the concentration of 20 μg/ml in the serum reduced medium. Cells were incubated for another 24 hours to allow the NPs to interact with cells and to induce differentiation mediated by NGF. Then

the cells were cultured for 1 day with 30 minutes of LED irradiation at the intensity of 1.90, 1.44 and 1.09 mW/cm^2 daily, respectively. Cells cultured without being treated by LED irradiation or NPs were considered as controls. During the LED irradiation, the temperature of the medium was recorded using the HH374 4-Channel Type K Data Logger Thermometer (OMEGA Engineering, Inc., Norwalk, CT). Finally, the neuronal differentiation of cells was observed and recorded using a light microscope (Axiovert 200 M Inverted Fluorescence/phase Contrast Microscope (Carl Zeiss, Inc. Jena, Germany) equipped with an AxioCam CCD camera). For each group, at least 40 pictures were acquired, and more than 4000 cells were quantified. The number of differentiated cells, the length and number of neurites in each image were counted and measured using the Simple Neurite Tracer as a plugin of Fiji.

Calcium imaging

PC-12 cells treated with NGF-SPIO-Au NPs of 20 μg/ml were incubated with the Fluo-4 direct calcium assay (Life Technologies) according to the manufacturer's protocol and with 5 mM probenecid as a stock solution. Briefly, 10 ml of calcium assay buffer and 200 μL of the 250 mM probenecid stock solution were mixed with the calcium reagent. The calcium reagent solution was then directly added to dishes containing cells in the growth medium in a 1:1 ratio. The dishes were then incubated for 60 minutes before fluorescence imaging. For the LED light stimulation, the calcium level was monitored immediately with the treatment of LED irradiation at the intensity of 1.90, 1.44 and 1.09 mW/cm^2. The group without LED irradiation was considered as a control. The Ca^{2+} signals of the PC-12 cells were captured by performing the real-time confocal imaging on Zeiss LSM 510 META NLO Two-Photon Laser Scanning Confocal Microscope System (Carl Zeiss, Inc. Jena, Germany) with 40 objectives under 488-nm laser excitation at the speed of 2 frames/second (512 × 512 pixel images). The measured fluorescence signals F were normalized to the baseline fluorescence intensity F_0 (10 s).

RNA extraction and reverse transcription-polymerase chain reaction (RT-PCR)

PC-12 cells were seeded in PLL pre-coated 6-well plates. After reaching confluency, cells were incubated with fresh serum-reduced medium with and without treatment with NGF-SPIO-Au NPs at the concentration of 20 μg/ml, respectively. Cells were then incubated for another 24 hours to allow the NPs to sufficiently interact with cells and to induce differentiation. Then the cells were cultured for 1 day with LED irradiation for 30 minutes at the intensities of 1.90, 1.44, and 1.09 mW/cm^2, respectively. Then, the total mRNA was extracted from PC-12 cells using the RNeasy® mini kit (Qiagen Sciences), according to the manufacturer's protocol. mRNA concentration of each sample was measured using a NanoDrop 2000c Spectrophotometer (NanoDrop Technologies, LLC, Wilimington, Delaware). All the mRNA samples were diluted to 10 ng/μl. Then the diluted mRNA samples were reverse-transcribed to complementary DNA by using a high capacity cDNA reverse transcription kit (Applied Biosystems) and followed by polymerase chain reaction (PCR) amplification using TaqMan® gene expression assays (Applied Biosystems) for integrin beta 1 (Rn00566727_m1) and tubulin beta 3 (Rn00594933_m1). The expression levels were recorded with respect to the control group (without LEDs) and were normalized to GAPDH (Rn01775763_g1).

Western blot analysis

Cells were treated according to the previous RT-PCR process. Total cell lysate was collected and prepared using Pierce® RIPA lysis and extraction buffer (Thermo Scientific) containing the cOmplete EDTA-free protease inhibitor (Millipore Sigma) (1 tablet for 10 ml lysis buffer). After lysing for 30 minutes on ice and then centrifuging at 14000×*g* for 15 minutes at 4 °C, the supernatant was collected. 2× Laemmli sample buffer (Bio-Rad) was added to the protein solution in a 1: 1 ratio and the protein solution was then heated to 95 °C for 5 min in order to denature the protein, and centrifuged at 16000×*g* for 1 minute at 4 °C. Then the samples were loaded onto Mini-PROTEAN® TGX™ Precast Protein Gels (Bio-Rad). After running the gel at 80 V for 5 minutes and 150 V for 1 hour, the proteins were transferred (90 V, 70 min) onto an Immun-Blot® PVDF Membrane (Bio-Rad). The membrane was then blocked for 60 minutes with the blocking buffer (1:1 Odyssey® blocking buffer in Tris-buffered saline (TBS) (LI-COR): 1x TBS). After blocking, the membrane was incubated overnight at 4 °C with β3-tubulin (Cell Signaling, 5666) and GAPDH (Invitrogen, PA1988) primary antibodies (at 1:1000), respectively. After washing 5 times with 0.05% Tween-20 in TBS for 5 minutes, the membranes were incubated for 1 hour at room temperature with StarBright™ Blue 700 Goat Anti-Rabbit IgG (12004158, Bio-Rad) diluted to 1:2500 (v/v). The membranes were washed 5 times again with 0.05% Tween-20 in TBS and 2 times with TBS. Finally, the labeled proteins were visualized by using the LI-COR Odyssey CLx Infrared Scanner (LI-COR Biosciences) and analyzed by using the ImageJ software.

Statistical analysis

All results were analyzed based on at least three independent experiments and presented as mean ± standard deviation. Statistical analysis was performed by using the analysis of variance (ANOVA) with Tukey post-hoc test to assess NGF-SPIO-Au treated and untreated cells with and without LED irradiation. A *P*-value less than 0.05 was considered as a significant difference.

Results

Our previous study has shown that our lab-synthesized SPIO-Au NPs with the diameter of 20.8 nm had quasi-spherical shape with narrow size distribution and excellent optical property. The successful functionalization of NGF to SPIO-Au NPs was confirmed through zeta potential measurements.[4] In the following experiments, we focused on exploring the synergistic effect of LED light and NGF-SPIO-Au NPs for promoted neuronal differentiation and neurite growth.

Cytotoxicity evaluation

The viability and proliferation evaluation of NGF-SPIO-Au NP-treated PC-12 cells irradiated by LED light was examined by measuring the absorbance of the formazan dye generated by the

reduction of water-soluble tetrazolium salt (WST-8) through dehydrogenases activities in cells, which was proportional to the number of living cells.[28] Our results show that without NGF-SPIO-Au NPs, the stand-alone LED exposure did not induce significant WST-8 reduction for up to 5 days of incubation, revealing the unaffected cellular proliferation by LED illumination alone (Figure 1). After 1 day of incubation with 20 μg/ml of NGF-SPIO-Au NPs, the LED exposure of 1 minute, 10 minutes, and 1 hour resulted in a slight decrease of WST-8 reduction (Figure 1, *A*). After 3 days of incubation, this decrease by LED effect was noticed at the NP concentration of 1, 5, 10, and 20 μg/ml (Figure 1, *B*). After 5 days of incubation, the decrease of WST-8 reduction was noticed at the concentrations of 5 and 10 μg/ml (Figure 1, *C*), indicating that the LED irradiation suppressed the promotional effect of NPs on cell proliferation. However, the synergistic effect of LEDs and NPs still resulted in a higher proliferation rates compared with the control groups without LEDs and NPs. Figure 1, *D* showed the time and concentration dependence of the WST-8 reduction with 30 minutes of LED exposure each day. Without NP-treatment, the PC-12 cells gained the highest WST-8 reduction rate after 5 days. However, the highest WST-8 reduction rate with NP-treatment was observed after 3 days, which might be explained by the fact that the existence of NPs largely promoted the WST-8 reduction and therefore cells reached confluency after 3 days of incubation.

To further explore the cytotoxic effect of LEDs at different light intensities with NGF-SPIO-Au NPs, the Trypan blue exclusion assay was performed. The results of the living cells to total cells ratio showed that after 1 day of incubation, the LED intensity increased from 1.09 to 1.90 mW/cm^2 induced a slight reduction of cell viability from 0.97 to 0.95 at the NP concentration of 5 μg/ml, while the cell viability of all LED intensities at NP concentrations from 0 to 20 μg/ml was still above 0.95, indicating no obvious cytotoxic effect of LEDs on PC-12 cells at this time point (Figure 2, *A*). After 3 days of incubation, only a slight reduction of cell viability was observed for the LED illumination of 1.90 mW/cm^2 at all NP concentrations (0–20 μg/ml, viability >89%) (Figure 2, *B*). After 5 days of incubation, the slight reduction of cell viability by using LED with stronger intensities was only observed at NP concentrations ≤10 μg/ml (Figure 2, *C*). At this point, the viability is recovered at NP concentrations of 20 μg/ml, confirming that LEDs had little long-term effect on viability at this concentration of NPs (Figure 2, *D*). To minimize the viability effect and maximize the stimulation effect of the LED light, it is recommended to use LEDs at higher intensity (i.e., 1.90 mW/cm^2) for a shorter time of incubation (i.e., 1 day) with higher concentrations of NPs (i.e., 20 μg/ml).

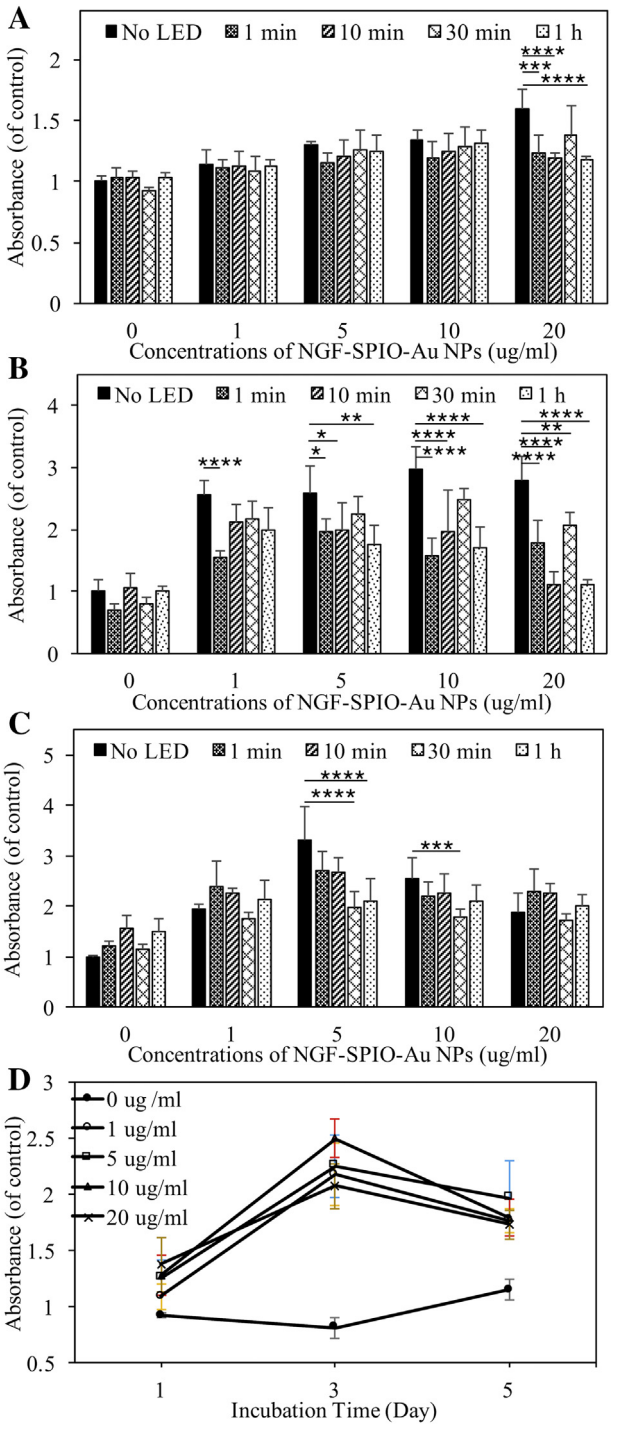

Figure 1. Cell viability evaluation by using a CCK-8 kit. PC-12 cells treated and untreated by NGF-SPIO-Au NPs for (A): 1 day, (B): 3 days and (C): 5 days of incubation with 0 minutes, 1 minute, 10 minutes, 30 minutes and 1 hour of LED exposure (1.90 mW/cm^2) daily; (D) the time and concentration dependency of absorbance value for cells exposed to 30 minutes of LED light (1.90 mW/cm^2) daily. *P < 0.05; **P < 0.01; ***P < 0.001, ****P < 0.0001.

Thermal effect of LED light

The temperature measurements in the cell culture medium under the LED light exposure from 0 to 1800 seconds showed that the LED irradiation elevated the local medium temperature after 30 minutes of LED exposure (Figure 3), while without LED light, this temperature elevation was not observed for both cases with and without NP treatment. The NPs treated medium temperature under the LED irradiation of 1.90 mW/cm^2 increased by 4.6 °C, while this value was 3.3 °C and 2.4 °C under the LED irradiation of 1.44 and 1.09 mW/cm^2, respectively. It is noticed that the temperature of the medium reached equilibrium after the LED irradiation of 1100 seconds. By comparing the temperature rise of LED irradiation at 1.90 mW/cm^2, it is found that the temperature

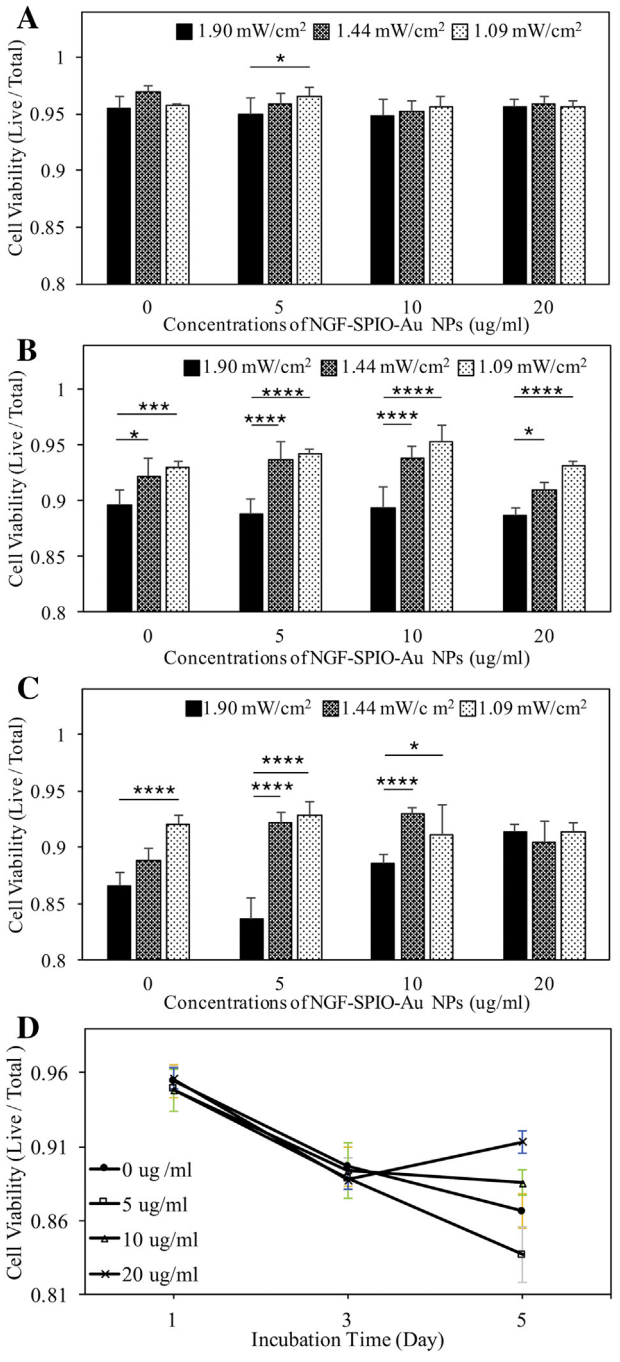

Figure 2. Cell viability evaluation by Trypan Blue staining. PC-12 cells treated and untreated by NGF-SPIO-Au NPs were irradiated with 30-minutes of LED light at 3 different intensities: 1.90, 1.44 and 1.09 mW/cm^2 daily for the (A): 1 day, (B): 3 days and (C): 5 days of incubation, (D) the time and concentration dependency of cell viability for cells exposed to 30 minutes of LED light (1.90 mW/cm^2) each day. *P < 0.05; **P < 0.01; ***P < 0.001, ****P < 0.0001.

rise of the NPs treated group (marked as "□" in Figure 3, total temperature increase is 4.6 °C) is higher than that of the group without NPs (marked as"×" in Figure 3, temperature increase is 3.5 °C), at the same LED irradiation intensity. This higher temperature increase is mainly due to the enhanced localized surface plasmon resonance (LSPR) effect of NGF-SPIO-Au NPs, as reported from our previous work[38]: a strong light absorbance

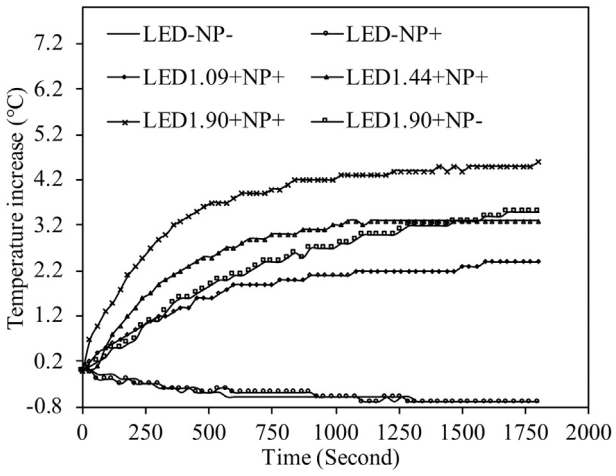

Figure 3. Temperature increase of cell culture media with and without plasmonic NGF-SPIO-Au NPs under the irradiation of LEDs or not. The temperature increase is higher at stronger LED intensity. The temperature rise of the NP-treated group is higher than that of the group without NPs at the LED irradiation of 1.90 mW/cm^2, confirming the photothermal effect of NGF-SPIO-Au NPs.

peak was observed at the wavelength of 525 nm, leading to the conversion of the photon energy to heat.

Morphology analysis

To examine the synergistic effect of LED light and NGF-SPIO-Au NPs on neuronal differentiation, PC-12 cells treated with NPs were exposed to LED light of different intensities for 30 minutes. PC-12 cells derived from rat pheochromocytoma respond to NGF by induction of the neuronal phenotype. Thus they have been widely used as a useful model to examine the neuronal differentiation.[39] The morphological differentiation of PC-12 cells in 5 different groups were recorded: LED-NP- (control group: no LED exposure, no NP treatment), LED-NP+ (no LED exposure, with NP treatment), LED1.90 (LED: 1.90 mW/cm^2, with NP treatment), LED1.44 (LED:1.44 mW/cm^2, with NP treatment) and LED1.09 (LED:1.09 mW/cm^2 LED exposure, with NP treatment).

To quantitatively investigate the level of neuronal differentiation, the number of differentiated cells and total cells were counted for each group. After 1 day of incubation, cells treated with NGF-SPIO-Au NPs and exposed to LED light showed a significant increase of the ratio of differentiated cells: for LED intensity at 1.90 mW/cm^2, this value reached 0.13, whereas for the control groups without LEDs or NP treatment, this value was only 0.07. LED light at lower intensities also led to an increase in differentiated cells (0.11 for LED at 1.44 and 1.09 mW/cm^2) in comparison with the control groups (Figure 4, *A*).

A similar trend was observed in examining the number of neurites per cells, as another parameter characterizing the level of neuronal differentiation: cells treated with NGF-SPIO-Au NPs and LED light developed more neurites per cell compared with the control groups without NPs or LED light. For the LED light intensities at 1.90, 1.44 and 1.09 mW/cm^2, the average number of neurites per cell is 1.58, 1.45 and 1.47, respectively, while it is 1.43 for the groups with only NPs and 1.21 for the control groups (Figure 4, *B*).

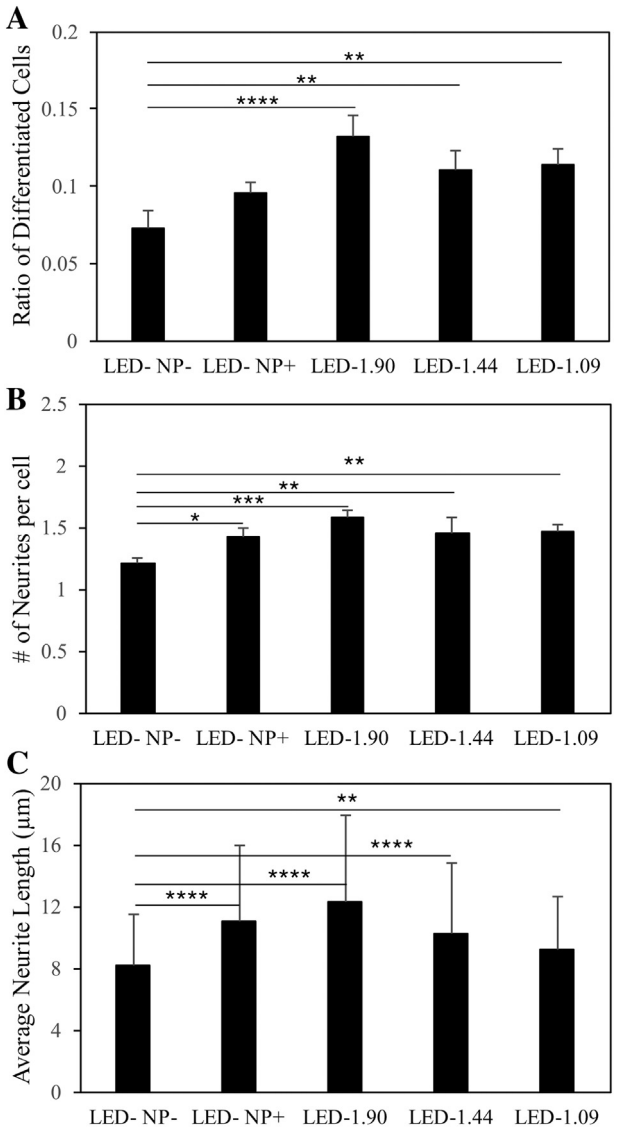

Figure 4. Morphology analysis for NGF-SPIO-Au NPs treated and untreated PC-12 cells exposed with and without LEDs. (A) Percentage of differentiated neuronal phenotype cells (B) Number of neurites per cell (C) Average neurite length. Group without LED or NPs were treated as control group. *$P < 0.05$; **$P < 0.01$; ***$P < 0.001$, ****$P < 0.0001$.

The neurites' length was also measured and quantified for examining the morphological changes of PC-12 cells. The groups treated with NPs and LED of 1.90 mW/cm^2 had the longest average neurite length of 12.24 μm, with an increase of about 51% (of control group). However, the groups with only NPs had an average neurite length of 11 μm (an increase of 35% of control group), indicating the synergistic effect of LED of 1.90 mW/cm^2 and NPs on promoting neurite growth, which was not observed at lower LED intensities (1.44 and 1.09 mW/cm^2) (Figure 4, *C*).

Localized Ca^{2+} signaling

To demonstrate whether the LED light could induce Ca^{2+} influx in differentiated PC-12 cells treated with NGF-SPIO-Au NPs, the localized Ca^{2+} signal was visualized using confocal fluorescence microscopy. Results showed no fluorescence intensity change for PC-12 cells without LED irradiation for both NPs treated and untreated cases, indicating no change of intracellular Ca^{2+} level (first, second, and fourth row) without the LED treatment, while an enhancement of the fluorescence intensities (red circle area) was observed for LED intensities at 1.90 and 1.44 mW/cm^2, indicating an increase of Ca^{2+} level stimulated by LED light (3rd and 5th row) (Figure 5, *A*). The F/F0 (normalized fluorescence by background fluorescence) in the red circle area was plotted in Figure 5, *B* (1st row), C (2rd and 3th row), D (4th and 5th row), and E (6th row). During the exposure of LED light at the intensities of 1.90 and 1.44 mW/cm^2, the fluorescence intensity was elevated from the base line, indicating the localized Ca^{2+} influx stimulated by LED light. On the other hand, neurons without LEDs exposure did not exhibit any elevation of the Ca^{2+} level from the base line for both the NP-treated and untreated cases.

Molecular effects

The RT-PCR and western blot assay were used to quantify the effect of LED light and NGF-SPIO-Au NPs on the expression level of the adhesive molecule, integrin β1, and the neural specific marker, β3-tubulin in PC-12 cells. The upregulation of the mRNA level of integrin β1 in PC-12 cells was observed in groups treated with LED light and NGF-SPIO-Au NPs as compared with the control groups (with NPs only). While without NPs, there was no significant change of mRNA level of integrin β1 in LED light irradiated PC-12 cells as compared with the control groups (no NPs and no LED irradiation) (Figure 6, *A*). These findings revealed that the synergistic effect of LED and NGF-SPIO-Au NPs enhanced the expression of integrin β1, which may be beneficial to the cell attachment and thus the induction of neurite growth.[40]

To account for the stimulation effect of LED and NGF-SPIO-Au NPs on neural differentiation, the mRNA levels of neural-specific marker, β3-tubulin were assayed. The results showed the upregulated expression of β3-tubulin in groups treated with LED and NPs at the intensities of 1.90 and 1.44 mW/cm^2 as compared with the control groups (with NPs only). However, without NPs, the groups exposed to LED light exhibited a slightly reduced expression level of β3-tubulin as compared with the control groups (no LED irradiation) (Figure 6, *B*).

This synergistic effect was also confirmed by the western blot analysis. The expression level of β3-tubulin protein was significantly upregulated by the LED (1.90 and 1.44 mW/cm^2) and NPs in comparison with the groups without LED and NPs, while the treatment of NPs alone or LED alone did not affect the expression level of β3-tubulin (Figure 6, *C* and *D*).

Discussion

There are plenty of previous works focused on using iron oxide NPs as the nano carrier of NGF to stimulate neurite outgrowth under the direction of external magnetic fields.[2,40–42] However, the high dose of iron oxide NPs was reported to cause cell dysfunction.[43–45] Too strong magnetic fields with long-time exposure have also been proven to be toxic to cells[46–48] and may suppress the reproductive process,[49,50] not to mention the other challenges of using bare iron oxide NPs like the aggregations.[5] In

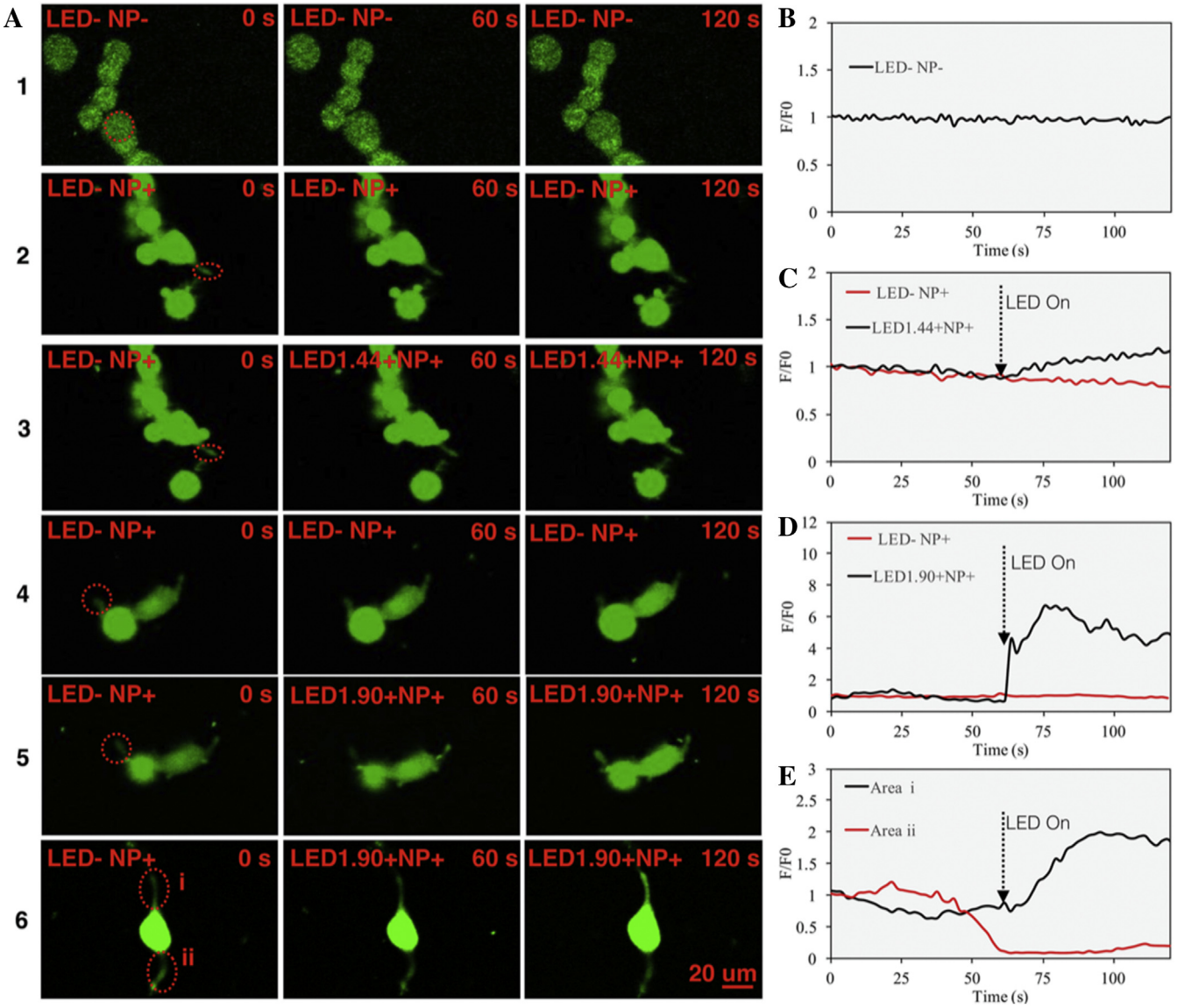

Figure 5. Calcium influx induced by LEDs at the neurites. (A). The first row shows control group of cells without LEDs and NPs; the second and fourth rows show groups of cells with NPs and without LED treatment. For the 3rd, 5th and 6th row, cells with NPs were irradiated by LED light at the intensity of 1.44, 1.09 and 1.90 mW/cm^2 starting from t = 60s to t = 120 s. (B). The normalized fluorescence intensity of circled area in the 1st row of (A) for the control group. (C) The normalized fluorescence intensity of circled area in the second and third rows of (A) for the NP treated group without LED and LED intensity = 1.44 mW/cm^2, respectively. (D). The normalized fluorescence intensity of circled area in the 4th and 5th row of (A) for the NP treated group without LED and LED intensity = 1.90 mW/cm^2, respectively. (E). The normalized fluorescence intensity of circled area i and ii in the 6th row of (A) for LED intensity = 1.90 mW/cm^2.

this work, we presented the exploration of using our lab-synthesized NGF-SPIO-Au NPs as a nanomedicine to regenerate neurons non-invasively through low-intensity LED illumination. We demonstrated that low-intensity LEDs (up to 1.90 mW/cm^2) can trigger the neurite growth and neuronal differentiation remarkably with a stimulation time up to 30 minutes for 1 day of incubation. Within this time period, LED light did not induce severe toxicity on PC-12 cells at the measured intensities (up to 1.90 mW/cm^2) and exposure time (up to 1 hour).

From the morphology evaluation, we demonstrated the intensity-dependence of neurite growth and neuronal differentiation of PC-12 cells treated by LED irradiated NPs. And the comparison between the group treated by NPs alone, and by LED-illuminated NPs showed that the synergistic effect of LED irradiation and NGF-SPIO-Au NPs is more effective than using NPs alone, which could be due to the remarkable photothermal effect of NPs from LED irradiation.

It is known that microtubules are essential cytoskeletal elements within the growth cones that affect the axon regeneration and outgrowth under the stimulation.[51] The associated microtubule proteins can be regulated by Ca^{2+} and/or Ca^{2+} sensitive kinases.[52] Filamentous actin (F-actin), as the other major cytoskeletal element within the growth cones, is also regulated by Ca^{2+} through affecting the binding affinity of various actin-binding proteins (ABP) to F-actin.[53] Therefore the concentration of cytoplasmic and intracellular Ca^{2+} has been treated as an essential regulator of

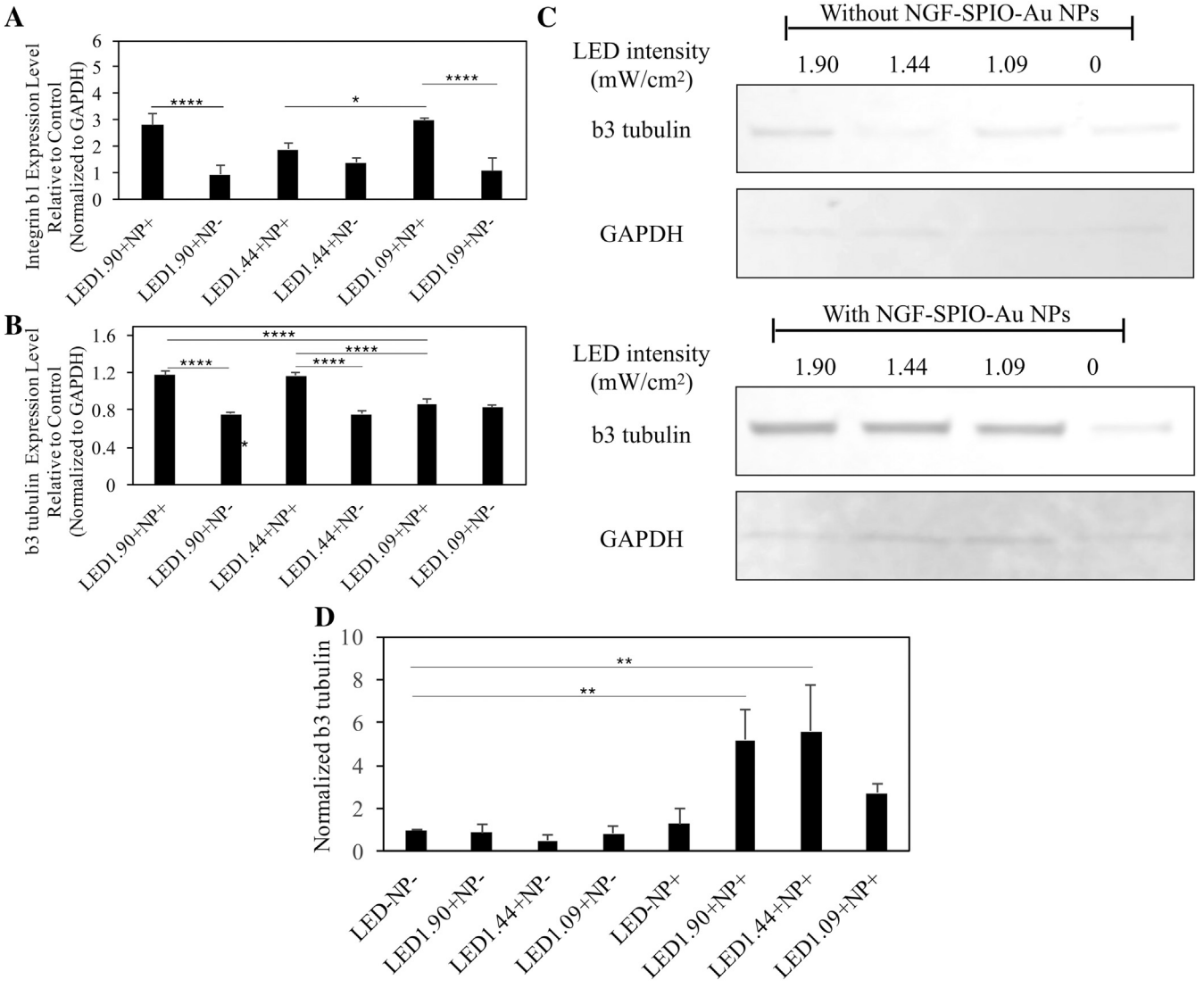

Figure 6. Results of RT-PCR and western blots for PC-12 cells treated with/without NGF-SPIO-Au NPs (20 μg/ml) and exposed to different intensity of LED light. (A) RT-PCR results for the mRNA level of integrin β1 of differentiated PC-12 cells. (B) RT-PCR for the mRNA level of β3-tubulin of differentiated PC-12 cells. The gene expression level was normalized to GAPDH as housekeeping gene. (C) Western blot analysis of β3-tubulin of differentiated PC-12 cells. (D) The average level of β3-tubulin protein normalized by GAPDH from triplicated experiments. *$P < 0.05$; **$P < 0.01$; ***$P < 0.001$, ****$P < 0.0001$.

neurite outgrowth, and the optimal range of Ca^{2+} can promote the neurite steering and extension.[54] Our results showed that the LED light-irradiated NPs induced a local Ca^{2+} influx in neurites, which implied the formation of the local calcium gradients that could interact with the growth cone cytoskeleton.[27]

In addition, we found from the molecular analysis that the stimulation by LED and NPs upregulated the neuronal specific marker as well as the cell adhesive molecules, which were associated with the cell attachment and neurite growth. And this stimulation effect was not found by LED or NPs alone. Additionally, the heat generation was observed during the LED irradiation of the NPs-treated medium which was the result of the LSPR effect of NGF-SPIO-Au NPs. These results suggest that the photostimulation of LED light might promote the neuronal differentiation and the neurite outgrowth via the photothermal effect of LED irradiated NGF-SPIO-Au NPs by modulating the local Ca^{2+} level and enhancing the cell attachment. However, it is still unclear that whether any other factors triggered by LED illumination on NGF-SPIO-Au NPs could affect the neuronal differentiation pathway. Therefore a more detailed investigation on exploring other neural-related factors is needed to further explore the mechanism of nerve regeneration, which will be the focus of our future study. Another limitation towards in vivo validation is the tissue penetration depth of 525 nm LED light. To overcome this, micro or nano-LED fibers can be used in future studies, which would allow the wireless optogenetic manipulation of neuronal activities in animals.[55,56]

In summary, this study reported a novel non-invasive neuroregeneration approach of using low-intensity LED light to irradiate NGF-SPIO-Au NPs, a promising nanomedicine, for promoting remarkable neuronal differentiation and neurite outgrowth in an intensity-dependent manner. And LEDs of

higher intensities were favored to produce more differentiated cells, more branching points and longer neurite length. No severe toxicity was observed upon LED light irradiation at our measured intensities. In particular, NGF-SPIO-Au NPs irradiated by LED light of 1.90 mW/cm^2 were found to induce the calcium influx in the neurites, and upregulate a neural differentiation specific marker, β3-tubulin, and an adhesive molecule integrin β1. The results demonstrated a promising non-invasive nanomedicine-based neurogenesis induction scheme using low-intensity LED irradiated NGF-SPIO-Au NPs for nerve regeneration.

Acknowledgments

This work was supported by the U.S. National Science Foundation CAREER program [grant number 1751435], the U. S. Department of Energy ARPA-E [grant numbers DE-AR0000531 and DE-AR0000945], the National Institutes of Health [grant numbers R01 AR 52379 and AR 61821), and the National Space Biomedical Research Institute through NASA Contract [grant number NCC 9-58]. The author would like to thank Central Microscopy Imaging Center at Stony Brook University for their technical support of fluorescence imaging.

References

1. Bodelon G, Costas C, Perez-Juste J, Pastoriza-Santos I, Liz-Marzan LM. Gold nanoparticles for regulation of cell function and behavior. *Nano Today* 2017;**13**:40-60.
2. Riggio C, Calatayud MP, Giannaccini M, Sanz B, Torres TE, Fernández-Pacheco R, et al. The orientation of the neuronal growth process can be directed via magnetic nanoparticles under an applied magnetic field. *Nanomed Nanotech Biol Med* 2014;**10**:1549-1558.
3. Marcus M, Karni M, Baranes K, Levy I, Alon N, Margel S, et al. Iron oxide nanoparticles for neuronal cell applications: uptake study and magnetic manipulations. *J Nanobiotechnology* 2016;**14**:37.
4. Yuan M, Wang Y, Qin Y-X. Promoting neuroregeneration by applying dynamic magnetic fields to a novel nanomedicine: superparamagnetic iron oxide (SPIO)-gold nanoparticles bounded with nerve growth factor (NGF). *Nanomed Nanotech Biol Med* 2018;**14**:1337-1347.
5. Yoffe S, Leshuk T, Everett P, Gu F. Superparamagnetic iron oxide nanoparticles (SPIONs): synthesis and surface modification techniques for use with MRI and other biomedical applications. *Curr Pharm Des* 2013;**19**:493-509.
6. Wang L, Park H-Y, Lim SII, Schadt MJ, Mott D, Luo J, et al. Core@shell nanomaterials: gold-coated magnetic oxide nanoparticles. *J Mater Chem* 2008;**18**:2629-2635.
7. Xu Z, Hou Y, Sun S. Magnetic core/shell Fe3O4/au and Fe3O4/au/ag nanoparticles with tunable plasmonic properties. *J Am Chem Soc* 2007;**129**:8698-8699.
8. Zhang S, Qi Y, Yang H, Gong M, Zhang D, Zou L. Optimization of the composition of bimetallic core/shell Fe2O3/au nanoparticles for MRI/CT dual-mode imaging. *J Nanopart Res* 2013;**15**:1-9.
9. Connor EE, Mwamuka J, Gole A, Murphy CJ, Wyatt MD. Gold nanoparticles are taken up by human cells but do not cause acute cytotoxicity. *Small* 2005;**1**:325-327.
10. Sood A, Arora V, Shah J, Kotnala RK, Jain TK. Multifunctional gold coated iron oxide core-shell nanoparticles stabilized using thiolated sodium alginate for biomedical applications. *Mater Sci Eng C* 2017;**80**:274-281.
11. Karamipour S, Sadjadi MS, Farhadyar N. Fabrication and spectroscopic studies of folic acid-conjugated Fe3O4@ au core–shell for targeted drug delivery application. *Spectrochim Acta A Mol Biomol Spectrosc* 2015;**148**:146-155.
12. Ghaznavi H, Hosseini-Nami S, Kamrava SK, Irajirad R, Maleki S, Shakeri-Zadeh A, et al. Folic acid conjugated PEG coated gold–iron oxide core–shell nanocomplex as a potential agent for targeted photothermal therapy of cancer. *Artificial cells, nanomedicine, and biotechnology* 2018;**46**:1594-1604.
13. Han L, Zhang Y, Zhang Y, Shu Y, Chen X-W, Wang J-H. A magnetic polypyrrole/iron oxide core/gold shell nanocomposite for multimodal imaging and photothermal cancer therapy. *Talanta* 2017;**171**:32-38.
14. Li J, Hu Y, Yang J, Wei P, Sun W, Shen M, et al. Hyaluronic acid-modified Fe3O4@ au core/shell nanostars for multimodal imaging and photothermal therapy of tumors. *Biomaterials* 2015;**38**:10-21.
15. Kukreja A, Kang B, Kim H-O, Jang E, Son HY, Huh Y-M, et al. Preparation of gold core-mesoporous iron-oxide shell nanoparticles and their application as dual MR/CT contrast agent in human gastric cancer cells. *Journal of industrial and engineering chemistry* 2017;**48**:56-65.
16. Sabale S, Kandesar P, Jadhav V, Komorek R, Motkuri RK, Yu X-Y. Recent developments in the synthesis, properties, and biomedical applications of core/shell superparamagnetic iron oxide nanoparticles with gold. *Biomater Sci* 2017;**5**:2212-2225.
17. Tsao JY, Schubert EF, Fouquet R, Lave M. The electrification of energy: long-term trends and opportunities. *MRS Energy & Sustainability* 2018;**5**.
18. Pattison PM, Tsao JY, Brainard GC, Bugbee B. LEDs for photons, physiology and food. *Nature* 2018;**563**:493.
19. Miesenböck G. Genetic methods for illuminating the function of neural circuits. *Curr Opin Neurobiol* 2004;**14**:395-402.
20. Marino A, Genchi GG, Mattoli V, Ciofani G. Piezoelectric nanotransducers: the future of neural stimulation. *Nano Today* 2017;**14**:9-12.
21. Yong J, Needham K, Brown WGA, Nayagam BA, McArthur SL, Yu A, et al. Gold-Nanorod-assisted near-infrared stimulation of primary auditory neurons. *Adv Healthc Mater* 2014;**3**:1862-1868.
22. Eom K, Kim J, Choi JM, Kang T, Chang JW, Byun KM, et al. Enhanced infrared neural stimulation using localized surface plasmon resonance of gold nanorods. *Small* 2014;**10**:3853-3857.
23. Lee JW, Jung H, Cho HH, Lee JH, Nam Y. Gold nanostar-mediated neural activity control using plasmonic photothermal effects. *Biomaterials* 2018;**153**:59-69.
24. Lavoie-Cardinal F, Salesse C, Bergeron É, Meunier M, De Koninck P. Gold nanoparticle-assisted all optical localized stimulation and monitoring of Ca2+ signaling in neurons. *Sci Rep* 2016;**6**.
25. Chen N, Tian L, Patil AC, Peng S, Yang IH, Thakor NV, et al. Neural interfaces engineered via micro-and nanostructured coatings. *Nano Today* 2017;**14**:59-83.
26. Paviolo C, Haycock JW, Yong J, Yu A, Stoddart PR, McArthur SL. Laser exposure of gold nanorods can increase neuronal cell outgrowth. *Biotechnol Bioeng* 2013;**110**:2277-2291.
27. Gasperini RJ, Pavez M, Thompson AC, Mitchell CB, Hardy H, Young KM, et al. How does calcium interact with the cytoskeleton to regulate growth cone motility during axon pathfinding? *Molecular and Cellular Neuroscience* 2017;**84**:29-35.
28. Yuan M, Wang Y, Qin YX. SPIO-au core–shell nanoparticles for promoting osteogenic differentiation of MC3T3-E1 cells: concentration-dependence study. *J Biomed Mater Res A* 2017;**105**:3350-3359.
29. Yeh NG, Wu C-H, Cheng TC. Light-emitting diodes—their potential in biomedical applications. *Renew Sustain Energy Rev* 2010;**14**:2161-2166.
30. Mills E. The specter of fuel-based lighting. *American Association for the Advancement of Science* 2005;**308**:1263-4.
31. Whelan HT, Smits Jr RL, Buchman EV, Whelan NT, Turner SG, Margolis DA, et al. Effect of NASA light-emitting diode irradiation on wound healing. *J Clin Laser Med Surg* 2001;**19**:305-314.
32. Rodrigues de Morais NC, Barbosa AM, Vale ML, Villaverde AB, de Lima CJ, Cogo JC, et al. Anti-inflammatory effect of low-level laser and light-emitting diode in zymosan-induced arthritis. *Photomed Laser Surg* 2010;**28**:227-232.

33. Barolet D. Light-emitting diodes (LEDs) in dermatology. *Cutan Med Surg* 2008;**27**:227-238.
34. Naeser MA, Saltmarche A, Krengel MH, Hamblin MR, Knight JA. Improved cognitive function after transcranial, light-emitting diode treatments in chronic, traumatic brain injury: two case reports. *Photomed Laser Surg* 2011;**29**:351-358.
35. Serafim KGG, de Paula Ramos S, de Lima FM, Carandina M, Ferrari O, Dias IFL, et al. Effects of 940 nm light-emitting diode (led) on sciatic nerve regeneration in rats. *Lasers Med Sci* 2012;**27**:113-119.
36. Stroh A, Tsai HC, Wang LP, Zhang F, Kressel J, Aravanis A, et al. Tracking stem cell differentiation in the setting of automated optogenetic stimulation. *Stem Cells* 2011;**29**:78-88.
37. Zhang Z, Tarone G, Turner DC. Expression of integrin alpha 1 beta 1 is regulated by nerve growth factor and dexamethasone in PC12 cells. Functional consequences for adhesion and neurite outgrowth. *J Biol Chem* 1993;**268**:5557-5565.
38. Yuan M, Wang Y, Hwang D, Longtin JP. Thermocouple-tip-exposing temperature assessment technique for evaluating photo-thermal conversion efficiency of plasmonic nanoparticles at low laser power density. *submitted to Review of Scientific Instruments* 2019.
39. Westerink RHS, Ewing AG. The PC12 cell as model for neurosecretion. *Acta Physiologica* 2008;**192**:273-285.
40. Kim JA, Lee N, Kim BH, Rhee WJ, Yoon S, Hyeon T, et al. Enhancement of neurite outgrowth in PC12 cells by iron oxide nanoparticles. *Biomaterials* 2011;**32**:2871-2877.
41. Pilakka-Kanthikeel S, Atluri VSR, Sagar V, Saxena SK, Nair M. Targeted brain derived neurotropic factors (BDNF) delivery across the blood-brain barrier for neuro-protection using magnetic nano carriers: an in-vitro study. *PLoS One* 2013;**8**e62241.
42. Marcus M, Skaat H, Alon N, Margel S, Shefi O. NGF-conjugated iron oxide nanoparticles promote differentiation and outgrowth of PC12 cells. *Nanoscale* 2015;**7**:1058-1066.
43. Pisanic Ii TR, Blackwell JD, Shubayev VI, Finones RR, Jin S. Nanotoxicity of iron oxide nanoparticle internalization in growing neurons. *Biomaterials* 2007;**28**:2572-2581.
44. Mahmoudi M, Hofmann H, Rothen-Rutishauser B, Petri-Fink A. Assessing the in vitro and in vivo toxicity of superparamagnetic iron oxide nanoparticles. *Chem Rev* 2011;**112**:2323-2338.
45. Yan H, Teh C, Sreejith S, Zhu L, Kwok A, Fang W, et al. Functional mesoporous silica nanoparticles for photothermal-controlled drug delivery in vivo. *Angew Chem Int Ed* 2012;**51**:8373-8377.
46. Miyakoshi J. Effects of static magnetic fields at the cellular level. *Prog Biophys Mol Biol* 2005;**87**:213-223.
47. Lai H, Singh NP. Magnetic-field-induced DNA strand breaks in brain cells of the rat. *Environ Health Perspect* 2004;**112**:687.
48. Hashish AH, El-Missiry MA, Abdelkader HI, Abou-Saleh RH. Assessment of biological changes of continuous whole body exposure to static magnetic field and extremely low frequency electromagnetic fields in mice. *Ecotoxicol Environ Saf* 2008;**71**:895-902.
49. Chernoff N, Rogers JM, Kavet R. A review of the literature on potential reproductive and developmental toxicity of electric and magnetic fields. *Toxicology* 1992;**74**:91-126.
50. Ramadan LA, Abd-Allah ARA, Aly HAA, Saad-El-Din AA. Testicular toxicity effects of magnetic field exposure and prophylactic role of coenzyme Q10 and L-carnitine in mice. *Pharmacol Res* 2002;**46**:363-370.
51. Dehmelt L, Halpain S. Actin and microtubules in neurite initiation: are MAPs the missing link? *Dev Neurobiol* 2004;**58**:18-33.
52. Redondo PC, Harper AGS, Sage SO, Rosado JA. Dual role of tubulin-cytoskeleton in store-operated calcium entry in human platelets. *Cell Signal* 2007;**19**:2147-2154.
53. Wang H-J, Wan A-R, Jauh G-Y. An actin-binding protein, LlLIM1, mediates calcium and hydrogen regulation of actin dynamics in pollen tubes. *Plant Physiol* 2008;**147**:1619-1636.
54. Henley J, M-m Poo. Guiding neuronal growth cones using Ca2+ signals. *Trends Cell Biol* 2004;**14**:320-330.
55. McCall JG, Kim T-i, Shin G, Huang X, Jung YH, Al-Hasani R, et al. Fabrication and application of flexible, multimodal light-emitting devices for wireless optogenetics. *Nat Protoc* 2013;**8**:2413.
56. Cao H, Gu L, Mohanty SK, Chiao JC. An integrated μLED optrode for optogenetic stimulation and electrical recording. *IEEE Trans Biomed Eng* 2012;**60**:225-229.